Invited Paper

Ligand-tuning of the Excitation Wavelength of a Solid State *E/Z* Isomerization: [Zn(TA)$_2$(2,2′-bipyridyl)] in a Supramolecular Framework

Shao-Liang Zheng,* Milan Gembicky, Marc Messerschmidt and Philip Coppens*
Department of Chemistry, State University of New York at Buffalo, Buffalo, New York, 14260-3000, USA.

The single-crystal-to-single-crystal (SCSC) *E*→*Z* photoisomerization of TA in the supramolecular solid CECR-[Zn(TA)$_2$(bpy)]·H$_2$O (CECR = *C*-ethylcalixresorcinarene, HTA = tiglic acid, and bpy = 2,2′-bipyridine, is induced by 458 nm light, indicating a red-shift of the photo-active wavelength on introduction of the aromatic bpy ligand compared with the previously studied reaction of CECR-[Zn(TA)$_2$(H$_2$O)$_2$]·4H$_2$O. Theoretical calculations show that the initial excitation involves the bipyridyl ligand, which acts as an intramolecular photosensitizer for the isomerization process. The reaction is topotactic and illustrated by photodifference maps.

Keywords: Photocrystallography; Ligand-tuning; Supramolecular framework; *E/Z* isomerization reaction.

INTRODUCTION

Photochemical *E/Z* photoisomerizations have received considerable attention as they trigger important physiological reactions. In photoactive yellow protein (PYP) for example, the *E/Z* isomerization of the *p*-coumaric acid chromophore triggers the conformational change of the protein which leads to the physiological response of marine organism to exposure to blue light.[1,2,3] Although the process has been the subject of extensive time-resolved diffraction studies, the limited resolution of protein diffraction, prevents atomic-resolution observation of the triggering reaction, thus providing an impetus for study of the reaction in smaller systems. But unlike intramolecular cyclizations[4,5] and many [2+2],[6] [4+4][7] photodimerizations, especially when initiated by illumination in the long wavelength tail of an absorption band,[8] *E/Z*-photoisomerizations in the solid state do usually not occur as *topotactic*, single-crystal-to-single-crystal (SCSC) reactions. However, when it is possible to embed photoactive molecules within cavities in framework supramolecular crystals, the crystal lattice is much less affected by the photoinduced molecular change and SCSC reaction become common.[9,10,11,12] We have reported a number of *E/Z*-photoisomerization of framework-embedded photo-reactive molecules.[13,14] They include tiglic acid (HTA, Scheme I), and tiglic acid ligated to Zn(II) as [Zn(TA)$_2$(H$_2$O)$_2$], both within a supramolecular framework composed of CECR (CECR = *C*-ethylcalix[4]resorcinarene). Both photo-isomerize without loss of crystallinity, allowing a detailed kinetic study of the progress of the SCSC reaction. As part of our investigations of SCSC *E/Z*-photoisomerizations in supramolecular environments we have now isolated [Zn(TA)$_2$(bpy)] (bpy = 2,2′-bipyridine) in the same framework, yielding crystals of composition CECR-[Zn(TA)$_2$(bpy)]·H$_2$O (**1**). The results show that the excitation wavelength of *E/Z*-photoisomerizations can be tuned by judicious variation of a co-ligand which remains unaltered in the final reaction prod-

Scheme I The structure of (a) CECR, and (b) HTA

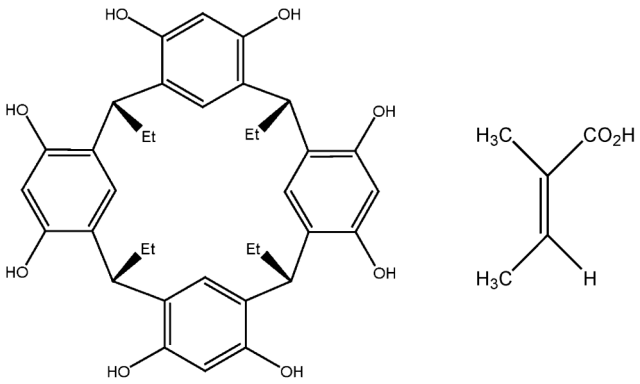

* Corresponding author. E-mail: coppens@buffalo.edu

ucts. Ligand-tuning of the absorption of metalloorganic complexes can be applied in optoelectrical and optomechanical switching.[15]

EXPERIMENTAL SECTION

Synthesis

1: Freshly prepared $Zn(OH)_2$ (0.05 mmol), HTA (0.1 mmol), bpy (0.05 mmol) and CECR (0.05 mmol) were mixed with benzene (1 mL) and water (2 mL) in a thick-walled tube. The sealed tube was allowed to stay at 100 ºC for 24 hours, followed by cooling to room temperature over 30 hours. Pale yellow crystals appeared during the cooling period.

X-Ray Crystallography and Photoreaction

Data on **1** were collected at 90 K on a *Bruker APEXII* CCD diffractometer installed at a rotating anode source ($Mo_{K\alpha}$ radiation, $\lambda = 0.71073$ Å), and equipped with an Oxford Cryosystems nitrogen flow apparatus. Data integration down to 0.82 Å resolution was carried out using *SAINT V7.34* with reflection spot size optimization. Absorption corrections were made with the program *SADABS*. The crystal was subsequently exposed for 4 hours at 90 K to 458 nm light from a 450 mW Ar laser. It was rotated around the ϕ axis during irradiation. X-ray data were collected at 90 K starting one hour after completion of the exposure. The parent structure was solved by direct methods and refined by least-squares methods against F^2 using *SHELXS-97* and *SHELXL-97*. In the parent structure non-hydrogen atoms were refined anisotropically, the hydroxy H atoms were located in a difference maps after which the riding model was applied. Other hydrogen atoms were positioned at idealized positions and refined in the same way. For the structure after irradiation, all non-hydrogen atoms of the product were located in Fourier difference maps, calculated with coefficients F_0(*exposed*)-F_0(*pre-exposure*), and then refined with restraints and constraints of the bond lengths and thermal parameters. The riding model was used for the hydrogen atoms. The percentage of the product in the crystal was treated as a variable in the refinements.

The 458 nm experiment was repeated with 325 nm light from a continuous 48 mW He/Cd laser and a second time with 355 nm light from a pulsed Nd vanadate laser with a repeat rate of 10 kHz.

Crystal data as well as details of data collection and refinement of **1** are described in Table 1, while Zn(II) coordination and hydrogen bonding distances are listed in Tables 2 and 3. The Fourier difference maps were produced with the *XD-2006* program package,[16] and the other drawings were produced with *Weblab Viewer Pro. 4.0*.[17] Full details can be found in CCDC-701070 - 701072, which can be obtained free of charge *via* http://www.ccdc.cam.ac.uk/conts/retrieving.html or deposit@ccdc.cam.uk (the Cam-

Table 1. Crystal data and structure refinement of **1**

	90 K (pre-exposure)	**90 K (exposed, 458 nm)**	**200 K**
Empirical formula	$C_{56}H_{64}N_2O_{13}Zn$	$C_{56}H_{64}N_2O_{13}Zn$	$C_{56}H_{64}N_2O_{13}Zn$
Formula weight	1038.46	1038.46	1038.46
Crystal system	Monoclinic	Monoclinic	Monoclinic
Space group	*P*2/c (No. 13)	*P*2/c (No. 13)	*P*2/c (No. 13)
a (Å)	18.6991(7)	18.7387(6)	18.8008(12)
b (Å)	11.2208(4)	11.1738(4)	11.2632(6)
c (Å)	28.5487(8)	28.6951(7)	28.7444(13)
α (°)	90	90	90
β (°)	121.859(2)	122.108(2)	122.054(3)
χ (°)	90	90	90
V (Å^3)	5087.6(3)	5089.3(3)	5158.9(5)
Z	4	4	4
μ ($Mo_{K\alpha}$)/mm^{-1}	1.356	1.355	1.337
Reflections collected	64517	42002	24094
Independent reflections	8971	8984	9089
R_{int}	0.0362	0.0252	0.0299
Goodness-of-fit on F^2	1.041	1.122	1.035
R_1 [$I > 2\sigma(I)$]	0.0390	0.0480	0.0404
wR_2 (all data)	0.1019	0.1225	0.1090
$\Delta\rho_{max}/\Delta\rho_{min}$ (e Å^{-3})	1.296/-0.753	0.986/-0.793	0.853/-0.527

Table 2. Hydrogen bonds distances in **1**

D–H···A	d(D..A)	<DHA	D–H···A	d(D..A)	<DHA
O(1)-H(1O)···O(8)	2.977(3)	173.9	O(6)-H(6O)···O(7)	2.788(3)	164.9
O(3)-H(3O)···O(2)	2.737(3)	168.5	O(7)-H(7O)···O(12)	2.701(2)	171.0
O(4)-H(4O)···O(10a)	2.730(2)	172.6	O(8)-H(8O)···O(9)	2.839(2)	165.8
O(5)-H(5O)···O(4)	2.769(2)	163.8			

a) -x,-y-1,z+1/2

Table 3. Interatomic distances (Å) in the Zn^{II} complex in **1** (B indicates an atom in the reaction product)

pre-exposure			
Zn(1)-N(1)	2.082(2)	Zn(1)-N(2)	2.056(2)
Zn(1)···O(9)	2.543(2)	Zn(1)-O(10)	2.016(2)
Zn(1)-O(11)	2.058(2)	Zn(1)-O(12)	2.272(2)
after exposure			
Zn(1)-N(1)	2.094(3)	Zn(1)-N(2)	2.037(3)
Zn(1)···O(9)	2.504(5)	Zn(1)-O(10)	2.037(6)
Zn(1)-O(11)	2.02(1)	Zn(1)-O(12)	2.258(6)
Zn(1)···Zn(1B)	0.273(8)		
Zn(1B)-N(1B)	2.06(1)	Zn(1B)-N(2B)	2.14(1)
Zn(1B)-O(9B)	1.97(3)	Zn(1B)-O(10B)	2.13(3)
Zn(1B)···O(11B)	2.34(6)	Zn(1B)-O(12B)	2.21(4)

bridge Crystallographic Data Center, 12 Union Road, Cambridge CB2 1EZ, UK; Fax: (+44) 1223-336-033).

Theoretical Calculations

Time-dependent density functional (TDDFT) calculations were performed at the B3LYP level, employing the Gaussian03 suite of programs.[18] The basis set used for N and H atoms was 6-31++G** while a LanL2DZ basis set with an effective core potential was employed for the Zn atom. Starting with the X-ray geometries, the structures were optimized by energy minimization.

RESULTS AND DISCUSSIONS

Crystal Structure

1 crystallizes in the monoclinic space group *P*2/c, with a 1:1 host-guest ratio (Table 1). The CECR molecules in **1** adopt the bowl-shaped (*r-cis-cis-cis*) conformation with four intramolecular hydrogen bonds along their upper rim [O···O = 2.730(2)-2.977(3) Å, Table 2, Fig. S1]. As shown in Fig. 1, two of the bowl-shaped symmetry-related molecules form a capsule with 7.1 × 6.5 Å effective cross section.[19] Two symmetry related [$Zn(TA)_2$(bpy)] molecules (symmetry code: 1-x, 1-y, 1-z) form a well-defined dimer, located in the capsule. Two adjacent bpy rings have an interplanar distance of 3.61 Å, whereas benzene rings of CECR are located at an interplanar distance of 3.56 Å from the bpy rings. As shown in Fig. 2, the Zn atom is 5-coordinate (Table 3) as one of the TA ligands is bidentate and the other is monodentate with one of the distances [Zn(1)··· O(9) 2.543(2) Å] exceeding the values typically found for Zn coordinated carboxylic acids (Zn-O 2.3 Å).[20] The TA ligands protrude from the cavities and are located in the channel along the *b* axis between the CECRs. The cavity volumes for the two TA ligands are 143.4 and 149.4 $Å^3$ respectively (Table 4). The [$Zn(TA)_2$(bpy)] molecules are further stabilized by hydrogen-bonds between TA and adjacent CECR molecules. One water molecule is included to fill the gap left in the channel.

Photoreaction

Absorption spectra of neat crystals of HTA, CECR

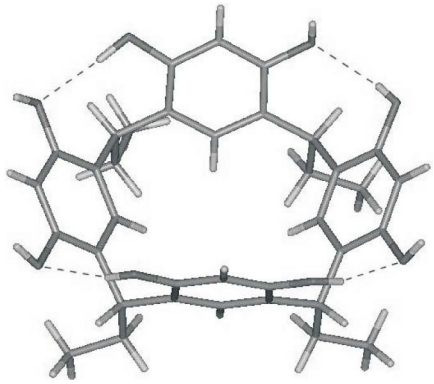

Fig. S1. CECR with intramolecular hydrogen bond connectivity of C_1 symmetry.

Fig. S2. Pictures of a crystal of **1.** Left: before, middle: during, and right: after exposure.

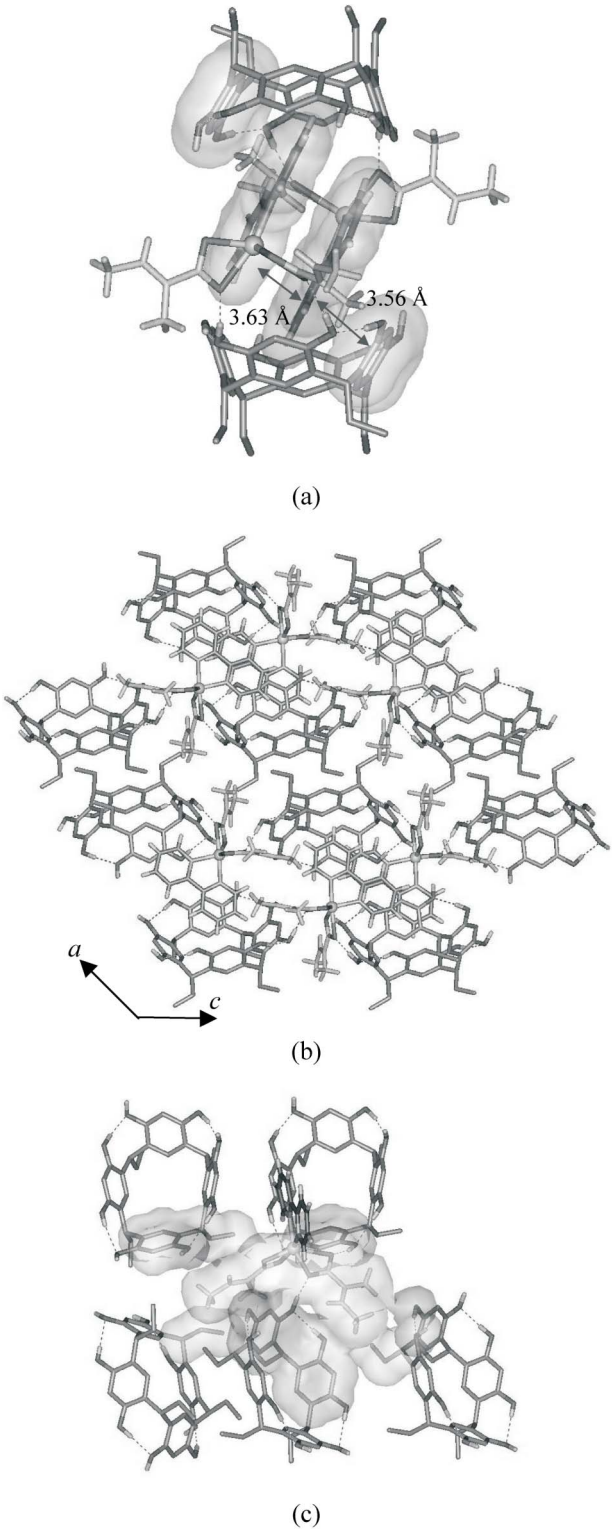

Fig. 1. Perspective views showing a) the $[Zn(TA)_2(bpy)]$ dimer in capsule-shaped cavity, b) packing diagram, and c) guest/host orbital interactions between the TA ligand in Zn compound and CECR in **1**. Surfaces shown are defined by the atomic vanderWaals radii.

and BPY are shown in Fig. 2. Compared with HTA, the absorption band of bpy is red-shifted by 100 nm. It has been shown that irradiation in the long wavelength tail of an absorption band can induce a SCSC photoreaction homogeneously throughout the entire volume of the crystal.[21] *E/Z*-photoisomerizations of HTA in CECR-HTA.2MeOH.1.5 H_2O and CECR-$[Zn(TA)_2(H_2O)_2].4H_2O$ have been triggered by 325 nm light from a 48 mW He/Cd laser. These and other *E/Z*-photoisomerizations that have been studied generally can not be induced with 458 nm light as produced by an Ar^+ laser. However, after replacement of the two water molecules by the 2,2′-bipyridyl ligand, 325 nm radiation from a 48 mW He/Cd laser does no longer introduce any features in the photodifference maps, even after exposure for 24 hours at 90 K.

In contrast, after exposure for 4 hours at 90 K with 458 nm light from a 450 mW Ar laser, photodifference maps show light-induced peaks corresponding to a conversion of part of the molecules to the *Z*-configuration (Figs. 3 and 4). Similar to CECR-$[Zn(TA)_2(H_2O)_2]\cdot4H_2O$, not only the migration of the methyl groups of the TA ligands but also diplacement of whole guest molecules is observed. The following shifts are of interest: Zn(1)-Zn(1B) 0.273(8) Å, Zn(1)-O(9) = 2.504(5) Å to Zn(1B)-O(9B) = 1.97(3) Å (B indicating the atom in the light-converted complex, O(9) being one of the oxygen atoms of the bidentate TA), Zn(1)-O(11) = 2.02(1) Å to Zn(1B)-O(11B) = 2.34(6) Å. Although the Zn atom is still 5-coordinate (Fig. 3), the coordination number of two TA ligands are interchanged, the bidentate TA becoming monodentate and vice versa.

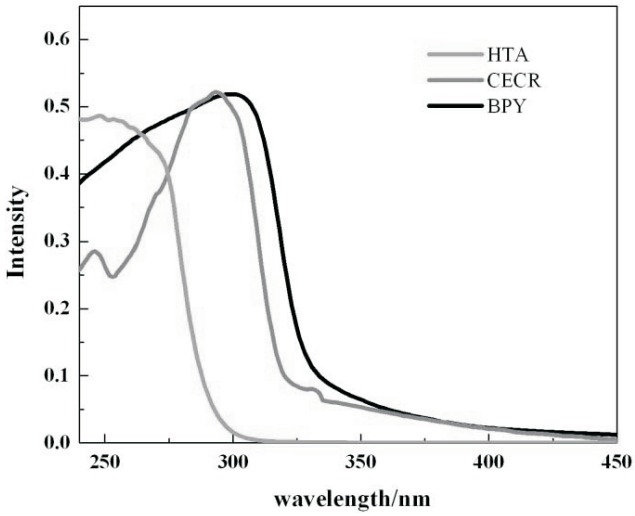

Fig. 2. Solid state UV-Vis reflectance spectra of HTA, CECR and bpy.

Table 4. Volume (Å^3) of the voids in **1**

	Unit cell volume (Å^3)	Volume (Å^3) of the space for guests per unit cell	Cavity volume per TA ligand (Å^3)	
pre-exposure	5087.6	2430.5 (47.8%)	143.4	149.4
after exposure	5089.3	2430.1 (47.7%)	157.8	162.7

Table 5. Calculated energy separations and oscilator strengths for intense transitions in HTA, $Zn(TA)_2$, and $Zn(TA)_2bpy$

Compound	Transition	*E*/eV (*f*)	Contour plots (isosurfaces at ±0.05 au) of the corresponding molecular orbital
HTA	HOMO to LUMO	6.0141 (0.359)	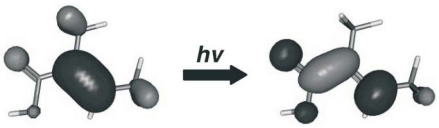
$Zn(TA)_2(H_2O)_2$	HOMO-5 to LUMO	5.581 (0.103)	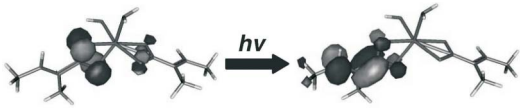
$Zn(TA)_2bpy$	HOMO-2 to LUMO+2	4.548 (0.163)	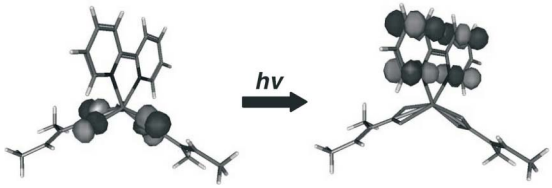

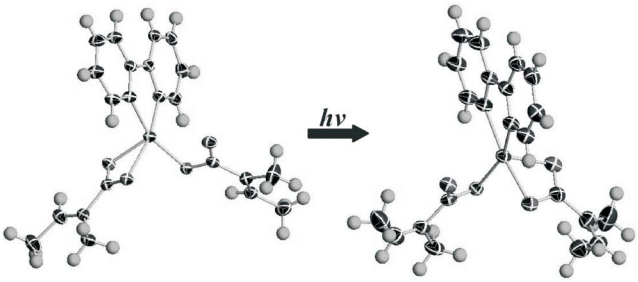

Fig. 3. Perspective views showing 50% probability displacement ellipsoids Zn compounds in **1** before exposure and after 4 hours exposure.

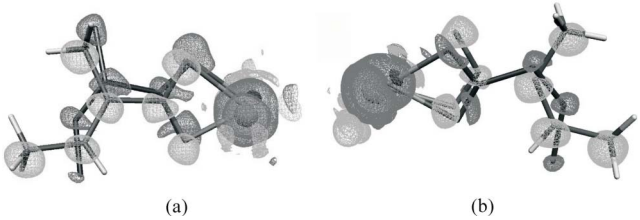

(a) (b)

Fig. 4. Photodifference maps of the two tiglic acid molecules in **1** after 4 hours exposure. Blue: 8.0, Gray: 0.8, Orange: -0.8, red: -8.0 e/Å^3.

Least squares refinement of the data after exposure indicates that 17.2(6) and 19.1(6) % of the two TA molecules repectively have converted to the *Z* form. No significant expansion of the unit cell (Table 1) was observed after exposure, the increment of the cavity size for per TA ligand is moderate (from 143.4 to 157.8 Å^3 and from 149.4 to 162.7 Å^3, Table 4) and less than that observed for the CECR-$[Zn(TA)_2(H_2O)_2]$ structure.[13]

Theoretical calculations of $[Zn(TA)_2(bpy)]$ confirm that excitations with significant oscilator strength correspond to ligand-to-ligand transfer (LLCT) from the TA to the bipyridyl ligand (Table 5).

CONCLUSIONS

We conclude that the photophysical properties of metalloorganic complexes are ligand-tunable. Thus, metal coordination and judicious choice of ligand allows selection of the wavelength with which a photochemical process can be inititated.

ACKNOWLEDGMENTS

Support of this work by the Petroleum Research Fund

of the American Chemical Society (PRF#43594-AC4) and the National Science Foundation (CHE0236317) is gratefully acknowledged.

Received September 10, 2008.

REFERENCES

1. Rajagopal, S.; Schmidt, M.; Anderson, S. I. H.; Moffat, K. *Acta Cryst.* **2004**, *D60*, 860.
2. Getzoff, E. D.; Gutwin, K. N.; Genick, U. K. *Nature Struct. Bio.* **2003**, *10*, 663.
3. Ihee, H.; Rajagopal, S.; Srajer, V.; Pahl, R.; Anderson, S.; Schmidt, M.; Schotte, F.; Anfinrud, P. A.; Wulff, M.; Moffat, K. *PNAS* **2005**, *102*, 7145.
4. See for example: Leibovitch, M.; Olovsson, G.; Scheffer, J. R.; Trotter, J. *J. Am. Chem. Soc.* **1997**, *119*, 1462; Leibovitch, M.; Olovsson, G.; Scheffer, J. R.; Trotter, J. *J. Am. Chem. Soc.* **1998**, *120*, 12755.
5. Turowska-Tyrk, I.; Trzop, E.; Scheffer, J. R.; Chen, S. *Acta Cryst.* **2006**, *B62*, 128.
6. Turowska-Tyrk, I. *Acta Cryst.* **2003**, *B59*, 670.
7. (a) Turowska-Tyrk, I.; Trzop, E. *Acta Cryst.* **2003**, *B59*, 779. (b) Kaftory, M.; Shteiman, V.; Lavy, T.; Schffer, J. R.; Yang, J.; Enkelmann, V. *Eur. J. Org. Chem.* **2005**, 847.
8. Abdelmoty, I.; Buchholz, V.; Di, L.; Guo, C.; Kowitz, K.; Enkelmann, V.; Wegner, G.; Foxman, B. M. *Cryst. Growth Des.* **2005**, *5*, 2210-2217.
9. MacGillivray, L. R.; Papaefstathiou, G. S.; Friscic, T.; Hamilton, T. D.; Bucar, D.-K.; Chu, Q.; Varshney, D. B.; Georgiev, I. G. *Acc. Chem. Res.* **2008**, *41*, 280-291.
10. (a) Hosomi, H.; Ohba, S.; Tanaka, K.; Toda, F. *J. Am. Chem. Soc.* **2000**, *122*, 1818. (b) Lavy, T.; Sheynin, Y.; Kaftory, M. *Eur. J. Org. Chem.* **2004**, 4802.
11. (a) Tanaka, K.; Toda, F.; Mochizuki, E.; Yasui, N.; Kai, Y.; Miyahara, I.; Hirotsu, K. *Angew. Chem., Int. Ed.* **1999**, *38*, 3523. (b) Tanaka, K.; Toda, F.; Mochizuki, E.; Yasui, N.; Kai, Y.; Miyahara, I.; Hirotsu, K. *Tetrahedron* **2000**, *56*, 6853.
12. (a) Arad-Yellin, R.; Brunie, S.; Green, B. S.; Knossow, M.; Tsoucaris, G. *J. Am. Chem. Soc.* **1979**, *101*, 7529. (b) Ananchenko, G. S.; Udachin, K. A.; Ripmeester, J. A.; Perrier, T.; Coleman, A. W. *Chem. Eur. J.* **2006**, *12*, 2441.
13. (a) Zheng, S.-L.; Messerschmidt, M.; Coppens P. *Chem. Commun.* **2007**, 2735. (b) Zheng, S.-L.; Messerschmidt, M.; Coppens P. *Acta Crystallogr.* **2007**, *B63*, 644.
14. Coppens P.; Zheng, S.-L.; Gembicky, M. *Z. Kristallogr.* **2008**, *223*, 265.
15. (a) Tong, Y. P.; Zheng, S. L.; Chen, X. M. *Inorg. Chem.* **2005**, *44*, 4270. (b) Zheng, S. L.; Chen, X. M. *Aust. J. Chem.* **2004**, *57*, 703.
16. Volkov, A.; Macchi, P.; Farrugia, L. J.; Gatti, C.; Mallinson, P.; Richter, T.; Koritsanszky, T. *XD2006-A Computer Program Package for Multipole Refinement, Topological Analysis of Charge Densities and Evaluation of Intermolecular Energies from Experimental and Theoretical Structure Factors*, 2006.
17. Weblab Viewer Pro. 4.0, Molecular Simulations Inc.: San Diego, CA., 1997.
18. Frisch, M. J.; Trucks, G. W.; Schlegel, H. B.; Scuseria, G. E.; Robb, M. A.; Cheeseman, J. R.; Zakrzewski, V. G.; Montgomery, J. A. Jr.; Stratmann, R. E.; Burant, J. C.; Dapprich, S.; Millam, J. M.; Daniels, A. D.; Kudin, K. N.; Strain, M. C.; Farkas, O.; Tomasi, J.; Barone, V.; Cossi, M.; Cammi, R.; Mennucci, B.; Pomelli, C.; Adamo, C.; Clifford, S.; Ochterski, J.; Petersson, G. A.; Ayala, P. Y.; Cui, Q.; Morokuma, K.; Malick, D. K.; Rabuck, A. D.; Raghavachari, K.; Foresman, J. B.; Cioslowski, J.; Ortiz, J. V.; Stefanov, B. B.; Liu, G.; Liashenko, A.; Piskorz, P.; Komaromi, I.; Gomperts, R.; Martin, R. L. D.; Fox, J.; Keith, T.; Al-Laham, M. A.; Peng, C. Y.; Nanayakkara, A.; Gonzalez, C.; Challacombe, M.; Gill, P. M. W.; Johnson, B.; Chen, W.; Wong, M. W.; Andres, J. L.; Gonzalez, C.; Head-Gordon, M.; Replogle, E. S.; Pople, J. A. *GAUSSIAN03, Revision C.02*; Gaussian, Inc.: Pittsburgh, PA, 2003.
19. Spek, A. L. *PLATON, A Multipurpose Crystallographic Tool*; Untrecht University: Utrecht, The Netherlands, 2003.
20. *International Tables for X-ray Crystallography, Vol. C*; Kluwer Academic Publishers: Dordrecht, Netherlands,1992; p 749.
21. Enkelmann, V.; Wegner, G.; Novak, K.; Wagener, K. B. *J. Am. Chem. Soc.* **1993**, *115*, 10390.